

## INNOVATIVE CLINICAL IMAGE

# Portal Vein Stenosis Following Liver Transplantation Hemodynamically Assessed with 4D-flow MRI before and after Portal Vein Stenting

Ryota Hyodo<sup>1\*</sup>, Yasuo Takehara<sup>1</sup>, Takashi Mizuno<sup>2</sup>, Kazushige Ichikawa<sup>2</sup>,  
Yasuhiro Ogura<sup>3</sup>, and Shinji Naganawa<sup>1</sup>

We present a case of a patient who underwent portal vein (PV) stenting for PV stenosis after a living-donor liver transplantation. A pretreatment 3D cine phase-contrast (4D-flow) MRI showed decreased, though hepatopetal, blood flow in the PV. After stenting, 4D-flow MRI confirmed an improvement in PV flow, with a more homogeneous flow distribution to each hepatic segment. 4D-flow MRI are valuable for understanding the hemodynamics of this area, planning for treatments, and evaluating the outcome of the interventions.

**Keywords:** 4D-flow MRI, living-donor liver transplantation, portal vein stenosis, portal vein stenting

## Introduction

Anastomotic portal vein (PV) stricture occasionally occurs as a post-operative complication of a living-donor liver transplantation (LDLT).<sup>1,2</sup> PV stenosis decreases portal venous blood supply to the liver graft and increases extrahepatic portal venous pressure, which may lead to liver dysfunction, splenomegaly, gastrointestinal bleeding, pancytopenia, intestinal edema, and ascites.<sup>1,3</sup> Since reoperations can be highly invasive for patients with severe post-operative adhesions, PV balloon angioplasty and stenting are preferred treatment options, with favorable long-term outcomes.<sup>3</sup> The hemodynamics of the portal system, however, have previously been identifiable only by direct angiography or portography.

Recently, time-resolved 3D cine phase-contrast (4D-flow) MRI has facilitated the cardiac phase-resolved iso-voxel acquisition of 3D blood flow velocity information within a 3D anatomical volume, throughout the cardiac cycle.<sup>4</sup> This technique also allows for simultaneous measurements of 3D flow velocity vectors in the PV system, including the

superior mesenteric vein (SMV), splenic vein (SV), and collateral circulations.<sup>5–8</sup> This case report is the first to describe the use of 4D-flow MRI analysis before and after percutaneous transhepatic PV stenting for assessment of a patient with PV stenosis after LDLT.

## Case Presentation

A 33-year-old female with biliary cirrhosis as a result of congenital biliary atresia was referred to our hospital for LDLT. Due to extremely severe adhesions and inflammatory changes around the native liver, the recipient's main PV trunk was fragile and unsuitable for PV reconstruction. Consequently, a right hepatic vein graft, which was obtained from the explanted native liver, was interposed to fill the gap between the recipient's healthy portion of the PV and the graft PV. During her post-operative follow-up, there was a progressing stenosis of the interposed vein graft. Using dynamic contrast-enhanced CT (DCE-CT) 69 days after LDLT, the entire length of the interposed vein graft showed severe stenosis (Supplementary Fig. 1). Therefore, further imaging was required for better understanding of hemodynamic information prior to interventional treatment.

After obtaining written informed consent, the Institutional Review Board approved 4D-flow MRI study, which was conducted using a clinical 3T MRI scanner (Prisma; Siemens AG Healthineers, Erlangen, Germany) with an 18 inch receiver coil. Following coronal balanced steady-state free precession (true fast imaging with steady-state precession [true-FISP]) imaging, a 3D axial dynamic contrast-enhanced MRI (Gd-3DMRA) was obtained for morphological imaging, using 0.1 mmol/kg of gadobutrol

<sup>1</sup>Department of Radiology, Nagoya University Graduate School of Medicine, Nagoya, Aichi, Japan

<sup>2</sup>Department of Medical Technology, Nagoya University Hospital, Nagoya, Aichi, Japan

<sup>3</sup>Department of Transplantation Surgery, Nagoya University Hospital, Nagoya, Aichi, Japan

\*Corresponding author: Department of Radiology, Nagoya University Graduate School of Medicine, 65, Tsurumaicho, Showa-ku, Nagoya, Aichi 466-8550, Japan. Phone: +81-52-744-2327, Fax: +81-52-744-2335, E-mail: ryouta771@med.nagoya-u.ac.jp

©2020 Japanese Society for Magnetic Resonance in Medicine

This work is licensed under a Creative Commons Attribution-NonCommercial-NoDerivatives International License.

Received: April 2, 2020 | Accepted: May 17, 2020

(Gadovist; Bayer, Leverkusen, Germany) and an injection rate of 1 mL/s. Subsequently, electrocardiogram-gated, respiratory navigator-gated, Cartesian trajectory, 4D-flow MRI was conducted covering the whole upper abdomen with the following parameters: coronal slab orientation, TR (ms)/TE (ms)/flip angle (°)/number of excitations: 17/2.9/8/1; *k*-space segmentation/temporal resolution (ms): 3/68; field of view (FOV, mm)/matrix: 300 × 300/208 × 208; slice thickness (mm)/number of slices: 1.5/60; voxel size (mm<sup>3</sup>): 1.4 × 1.4 × 1.5; velocity encoding (cm/s): 80; an acceleration factor with generalized autocalibrating partially parallel acquisition: 3; acceptance ratio (%): 95. The approximate acquisition time was 9 min. Data were reconstructed to 20 time frames per R-R intervals. The 4D-flow data set, segmented by true-FISP images which showed better visualization than Gd-3DMRA, was post-processed using a dedicated flow analysis software program (iTFlow; Cardio Flow Design, Tokyo, Japan). The software shows whole the blood flow vectors in the FOV, including the PV, SMV, SV, and the hepatofugal collateral circulations,

including the coronary vein, using various depictions of blood flow (i.e., 3D vector fields, streamlines, pathlines, and particle traces). The portal flowmetries were performed by placing a region of interest on the cross-sections of the main trunk and each segmental branch.

On the streamline and pathline images, which traced the movements of flow particles, the stenotic hepatic vein graft could not be visualized with the limited spatial resolution of the MRI (Fig. 1 and Supplementary Fig. 2). Although PV blood flow was reduced, antegrade PV blood flow was observed in the segments upstream and downstream of the severe stenotic segment. The calculated portal flow was 6.6 mL/s at the site upstream of the PV stenosis (Fig. 1). Evaluation of the splanchnic venous circulation revealed that the dilated coronary vein was a hepatofugal collateral circulation, though both the SMV and proximal SV flows were identified to be hepatopetal (Supplementary Fig. 2). Furthermore, analysis of the intrahepatic portal flow demonstrated post-stenotic dilation of the anterior branch of the PV, with clear visualization of vortex and helical flows inside the

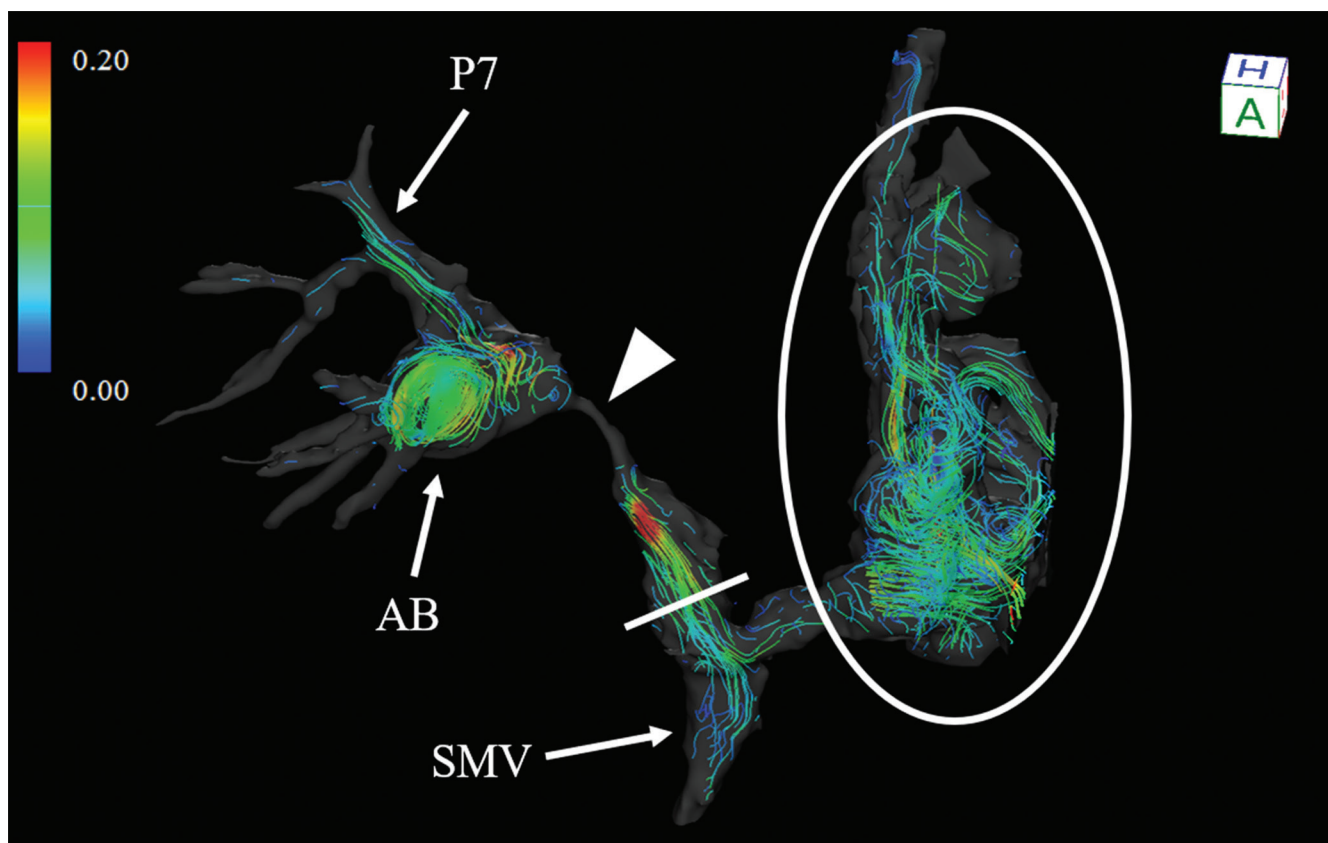


**Fig. 1** Streamline analysis utilizing the velocity data obtained by 3D cine phase-contrast (4D-flow) MRI before the intervention. Severe stenosis was observed in the main portal trunk (arrowhead), and an increase in blood flow immediately before the stenosis was observed (encoded red portion). The flow volume of the portal trunk was 6.6 mL/s upstream of the stenosis (measured at the line). The coronary vein (inside the circle) was developed, and hepatofugal flow was observed inside. Post-stenotic dilation and vortex flow were observed in the anterior branch. P7 blood flow was relatively maintained, while the flow in other portal branches was reduced in volume. 4D-flow, 3D cine phase-contrast; AB, anterior branch of the portal vein; P7, posterior superior branch of the portal vein; SMV, superior mesenteric vein.

dilated vessel cavity. The blood flow of posterior superior branch of the portal vein (P7) was relatively maintained, though the blood flows of the other intrahepatic PV branches were reduced, and the distribution of blood flow to those branches was disproportional (Table 1 and Supplementary Table 1).

On the interventional procedure, both the 0.035-inch guidewire and the 4-Fr catheter were passed through the stenotic portion without any resistance and proceeded to the SMV. Digital subtraction angiography (DSA) from the SMV showed considerable stenosis of the PV, which anatomically coincided with the location of the PV graft, and reduced opacity of the liver parenchyma (Supplementary Fig. 3A). There was a reflux of the contrast media to the SMV branches, without visualization of the SV, suggesting that the splenic flow was antegrade and supporting the findings of the pre-interventional 4D-flow MRI. Following predilatation, a 12 × 60-mm self-expandable stent (Epic vascular stent; Boston Scientific, Marlborough, MA, USA) was deployed. A DSA from the SMV revealed a normalized caliber of the PV, homogeneous opacity of the liver parenchyma, and disappearance of the SMV reflux (Supplementary Fig. 3B).

4D-flow MRI performed the next day in the same fashion as before the intervention but segmented by Gd-3DMRA showed adequate dilation and laminar antegrade blood flow at the stenotic site of the main PV (Fig. 2 and Supplementary Fig. 4). The portal flow rate at the main PV trunk was increased to approximately 26.6 mL/s. The coronary vein was patent after the intervention; however, the flow velocity inside the coronary vein was dramatically decreased, and the flow pattern turned to-and-fro over the cardiac cycle. The vortex flow in the dilated anterior branch of the PV was

**Table 1** Flow volume of portal venous branches before and after stent placement

	P5	P6	P7	P8a	P8b + c
Pre (mL/s)	0.24	0.20	2.14	0.23	0.03
Post (mL/s)	2.47	1.33	8.64	2.88	5.22

P5, anterior inferior branch of the portal vein; P6, posterior inferior branch of the portal vein; P7, posterior superior branch of the portal vein; P8, anterior superior branch of the portal vein.

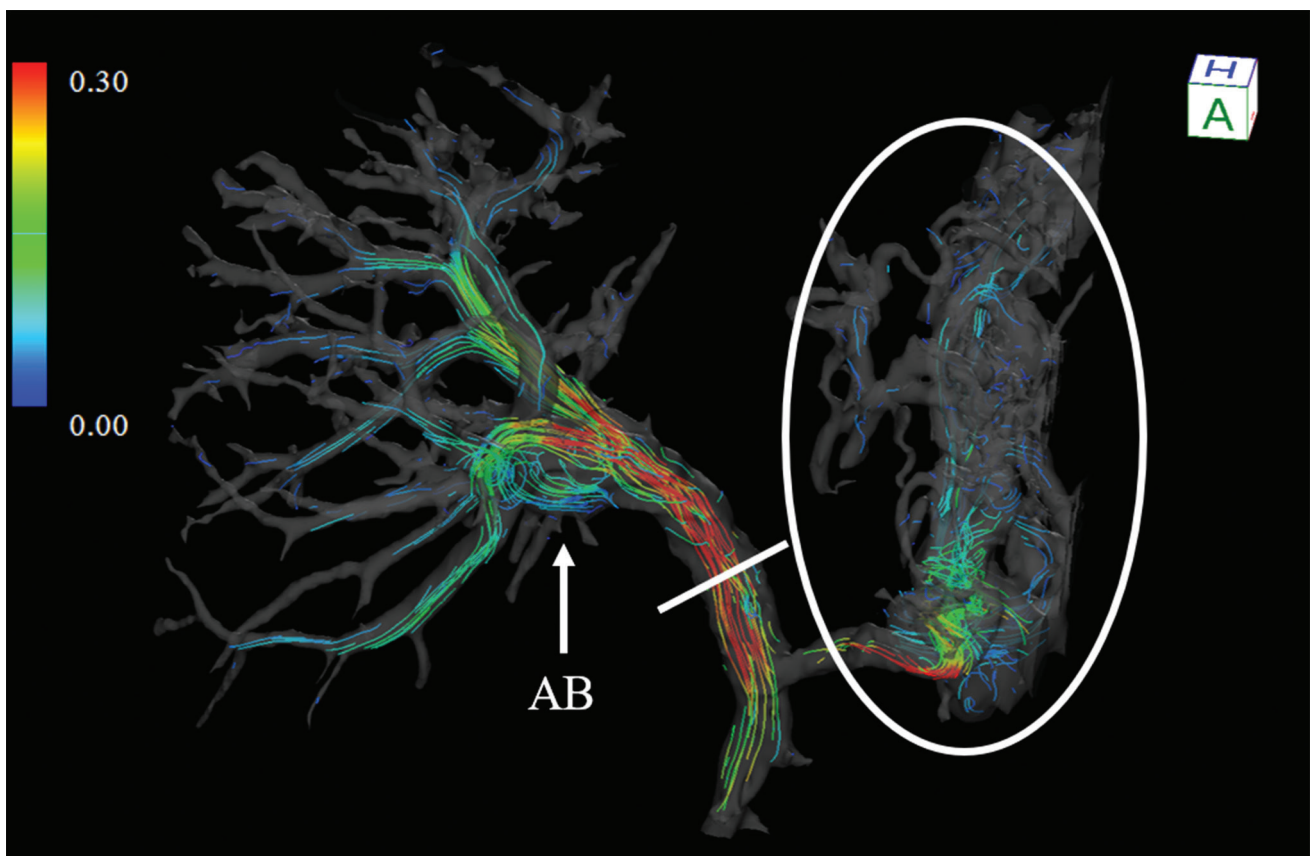


**Fig. 2** Streamline analysis using 4D-flow MRI after stent placement. High blood flow was observed in the main portal trunk, with a flow volume of 26.6 mL/s (measured at the line). Blood flow in the intrahepatic portal branches was homogeneously increased, with inconspicuous vortex flow in the anterior branch (arrow) and an improvement in blood flow disproportionality to each segmented portal vein. The blood flow in the coronary vein was markedly reduced (inside the circle), which reflected an improvement of portal hypertension. 4D-flow, 3D cine phase-contrast; AB, anterior branch of the portal vein.

inconspicuous, and the flow volume for each branch, which had been uneven before the intervention, was uniformly increased, with a laminar flow pattern (Table 1 and Supplementary Table 1). Doppler ultrasonography (US) also confirmed the improved hemodynamics of the PV trunk and the anterior branch of the PV.

Immediately after treatment, the patient regained her appetite. CT imaging performed 9 days after the intervention revealed patency of the PV stent and uniformly opacified intrahepatic PV branches with normalized calibers. Thrombocytopenia was also improved, and the patient was discharged 20 days after the interventional procedures.

## Discussion

In the present case, pre-interventional DCE-CT revealed severe stenosis or occlusion of the portion of the main PV trunk interposed by the recipient hepatic vein graft. We were, therefore, concerned about the feasibility of passing a guidewire through the narrowed segment. Information obtained via the pre-interventional 4D-flow MRI, however, revealed hepatopetal blood flow in the main trunk downstream of the stenosis, as well as upstream at the SMV and SV. Based on this information, the intervention was carefully planned and, consequently, a guidewire and 4-Fr catheter were successfully passed through the narrowed segment without resistance. While the stenosis of the main PV and the vortex flow in the dilated anterior portal branch were identified using Doppler US before the intervention, hemodynamic information related to the SV was only obtained by the 4D-flow MRI analysis. The advantages of 4D-flow MRI usage include its ability to provide quantitative and qualitative hemodynamic information in the entire FOV.<sup>5-8</sup> Furthermore, unlike Doppler US, retrospective flowmetry is a unique capability of 4D-flow MRI. Even after a patient leaves the MR suite, flow analysis can be repeated using the 4D data set.

In the present case, disproportionate blood flow delivery to different hepatic segments was observed before the intervention. The jet flow through the stenosed segment, followed by the vortex flow in the post-stenotic dilation of the anterior PV branch, hindered normal laminar blood flow delivery to all hepatic segments except S7. The vortex flow in the anterior PV branches subsided after the portal vein stenting, which uniformly normalized the blood flow distribution to the peripheral PV branches. To the best of our knowledge, there have been no previous reports of this technology being used to evaluate interventions that improve hepatic segmental blood flow distribution after liver transplantation.

In Table 1, we showed the blood flow volume of the main portal branches; however, the sum of the flow volume of the branches was smaller than the flow volume of the main PV. The reason is that the several small portal branches that were difficult to evaluate in terms of spatial resolution were not contained.<sup>7</sup> In addition, the pre-interventional 4D-flow

MRI showed vortex flow in the anterior branch of the PV, possibly leading to underestimate the blood flow volume of the peripheral branch of the anterior branch. The disadvantage of 4D-flow MRI is that the spatial resolution is still low compared with 2D phase contrast method and US, and is susceptible to the partial volume effect.<sup>9</sup> In addition, 4D-flow MRI requires long imaging time under free breathing, which causes blurring due to respiration even when respiratory-gated is performed. They sometimes make it difficult to evaluate small branches. In the present case, clinically useful images were obtained; however, it is necessary to improve the spatial and the temporal resolution in the future.

## Conclusion

We report the first usage of 4D-flow MRI hemodynamic evaluations before and after an interventional procedure in a patient with a PV stricture complication. 4D-flow MRI technique may be a feasible option for quantitative and qualitative assessments of intra- and extrahepatic PV blood flow dynamics before and after interventions in LDLT patients, with potential applications to many different kinds of vascular hemodynamic evaluations.

## Acknowledgments

The authors thank Y. Kato, R.T., Y. Sakurai, R.T and S. Abe, R.T. for their technological assistances in image acquisitions, and Komori Y. Siemens Healthcare for providing pre-product version of 4D-flow MR application. This work was supported by JSPS KAKENHI Grant Number JP19K17165.

## Conflicts of Interest

The second author Yasuo Takehara is an endowed chair of Nagoya University supported by a private company Himedic Nagoya; however, the status is irrelevant to the contents of this paper. The other authors have no conflicts of interest to disclose.

## Supplementary Information

Supplementary files below are available online.

### Supplementary Fig. 1

(A) Coronal and (B) axial contrast-enhanced computed tomography imaging demonstrated a severely stenosed segment of the main portal trunk (arrows), which corresponded to the interposed vein graft.

### Supplementary Fig. 2

3D vector analysis utilizing the velocity data obtained by 4D-flow MRI before the intervention. Antegrade blood flow was observed in the splenic vein downstream from the origin of the coronary vein (arrow). 4D-flow, 3D cine phase-contrast.

**Supplementary Fig. 3**

Interventional treatment by an ultrasound-guided percutaneous transhepatic approach. (A) DSA before the balloon angioplasty. The main portal trunk was severely stenotic (arrowhead), and the opacity of the liver parenchyma was reduced. Note that there was less opacity in the portal branches (arrows) than in the superior branches. The CM injected at the SMV showed numerous collaterals but no reflux to the splenic vein, which was consistent with the 4D-flow MRI findings before the intervention. Breaking through the stenosis was easy. (B) DSA after stent placement. The calibers of the portal veins (arrowhead) and the opacity of the liver parenchyma were improved (arrows). The CM injected at the SMV showed no collaterals. 4D-flow, 3D cine phase-contrast; CM, contrast media; DSA, digital subtraction angiography; SMV, superior mesenteric vein.

**Supplementary Fig. 4**

3D vector analysis using 4D-flow MRI after stent placement. The flow pattern of coronary vein turned to-and-fro. 4D-flow, 3D cine phase-contrast.

**Supplementary Table 1**

Average flow velocity of portal venous branches before and after stent placement

**References**

1. Craig EV, Heller MT. Complications of liver transplant. *Abdom Radiol (NY)* 2021; 46:43–67.
2. Delgado-Moraleda JJ, Ballester-Vallés C, Marti-Bonmati L. Role of imaging in the evaluation of vascular complications after liver transplantation. *Insights Imaging* 2019; 10:78.
3. Cheng YF, Ou HY, Tsang LL, et al. Vascular stents in the management of portal venous complications in living donor liver transplantation. *Am J Transplant* 2010; 10:1276–1283.
4. Markl M, Chan FP, Alley MT, et al. Time-resolved three-dimensional phase-contrast MRI. *J Magn Reson Imaging* 2003; 17:499–506.
5. Motosugi U, Roldán-Alzate A, Bannas P, et al. Four-dimensional flow MRI as a marker for risk stratification of gastroesophageal varices in patients with liver cirrhosis. *Radiology* 2019; 290:101–107.
6. Frydrychowicz A, Landgraf BR, Niespodzany E, et al. Four-dimensional velocity mapping of the hepatic and splanchnic vasculature with radial sampling at 3 tesla: a feasibility study in portal hypertension. *J Magn Reson Imaging* 2011; 34:577–584.
7. Bannas P, Roldán-Alzate A, Johnson KM, et al. Longitudinal monitoring of hepatic blood flow before and after TIPS by using 4D-flow MR imaging. *Radiology* 2016; 281:574–582.
8. Parekh K, Markl M, Rose M, Schnell S, Popescu A, Rigsby CK. 4D flow MR imaging of the portal venous system: a feasibility study in children. *Eur Radiol* 2017; 27:832–840.
9. Stankovic Z, Csatar Z, Deibert P, et al. Normal and altered three-dimensional portal venous hemodynamics in patients with liver cirrhosis. *Radiology* 2012; 262:862–873.